Design and Analysis of an Efficient Boost Converter for Renewable Energy Sources

Nisha Singh[*], S. P. Phulambrikar[**]

[*] Dept. of Electrical Engineering, SATI, Vidisha, Madhya Pradesh, India
[**] Associate Professor & HOD, Dept. of Electrical Engineering, SATI, Vidisha, Madhya Pradesh, India

Abstract- Renewable energy is evolved from natural sources. Photovoltaic (PV) and fuel cells are commonly used Renewable energy sources. A derived DC-DC converter is suggested for efficient renewable energy sources. An efficient Boost converter (BC) topology is discussed in this paper for renewable energy sources. The merits of this topology are reduced EME (Electromagnetic emission), fast transient response and low input current ripple. In suggested topology, 2 identical inductors and an auxiliary inductor are used to reduce the switching loss and switching stress of BC connected with PV system, used PWM technique for triggering the switches. The performance of BC along with PV system is analyzed by Matlab/Simulation software.

Index Terms- DC-DC Converter, EME, PWM technique.

I. INTRODUCTION

Boost converters are popularly employed in equipments for different applications. Boost converters are usually applied as pre-regulators or even integrated with the latter stage circuits or rectifiers into single-stage circuits [1][2]. Most renewable power sources, such as photovoltaic and fuel cell have quite low voltage output and require series connection or a voltage booster to provide enough voltage output.

Several soft-switching techniques, gaining the features of zero-voltage switching (ZVS) or zero-current switching (ZCS) for DC-DC converters, have been proposed to substantially reduce switching losses, hence, attain high efficiency at increased frequencies. There are many resonant or quasi-resonant converters with the advantages of ZVS or ZCS[7]. The main problem with these kinds of converters is that the voltage stresses on the power switches are too high in the resonant converters. Passive snubbers achieving ZVS are attractive [3]-[4], since no extra active switches are needed, and therefore, feature a simpler control scheme and lower cost.

Converters with interleaved operation are fascinating techniques nowadays. An interleaved converter with a coupled winding is proposed to a provide a lossless clamp [5]. Additional active switches are also appended to provide soft -switching characteristics. These converters are able to provide higher output power and lower output ripple.

This paper focus on soft switching technique for an efficient boost converter composed of two shunted elementary boost conversion units and an auxiliary inductor[6]. This system is able to turn on both the active power switches at zero voltage to reduce their switching losses and evidently raise the conversion efficiency. Since the two parallel operated boost units are similar, operation analysis and design for the converter module becomes quite simple. The simulation results show that this converter module performs very well with the output efficiency as high as 97%.

II. PHOTOVOLTAIC SYSTEM AND EFFICIENT BOOST CONVERTER CIRCUIT CONFIGURATION

Solar cells produce current when sunlight falls on them. In this paper the solar cell is simulated for any ambient temperature, sun light intensity and other internal parameters. An equivalent circuit is developed for easy analysis of solar cell. The PV cell is a electrical device, which produces electrical power when exposed to sunlight and they are connected to boost converter. In proposed model the current is considered as controlled constant current source, and the voltage changes based on the irradiation level. So the equivalent model contains a constant current source. The equivalent model is shown in Fig 1.

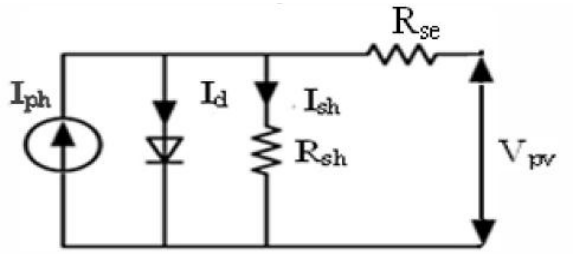

Fig 1. Equivalent Circuit for a Solar Cell

From the equivalent circuit, the current produced by the solar cell is given by,

$$I = I_L - I_D - I_{SH} \quad (1)$$

where,

I = Output current (Amperes)
I_L = Photo generated current (Amperes)
I_D = Diode current (Amperes)
I_{SH} = Shunt current (Amperes)

The current through these elements is governed by the voltage across them,

$V_j = V + IR_S$ (2)

where,

V_j = Voltage across both diode and resistor R_{SH} (Volts)
V = Voltage across the output terminals (Volts)
I = Output current (Amperes)
R_S = Series resistance (Ω)

By the Shockley diode equation, the current diverted through the diode is,

$$I_D = I_O\left\{exp\left[\frac{qV_j}{nkT}\right] - 1\right\} \quad (3)$$

where,
I_O = Reverse saturation current (Amperes)
n = Diode ideality factor (1 for an ideal diode)
q = Elementary charge
k = Boltzmann's constant
T = Absolute temperature

By Ohm's law, the current diverted through the shunt resistor is,

$$I_{SH} = \frac{V_j}{R_{SH}} \quad (4)$$

Substituting these into the Equation (1) produces the characteristic equation of a solar cell, which gives solar cell parameters to the output current and voltage,

$$I = I_L - I_O\left\{exp\left[\frac{q[V+IR_S]}{nkT}\right] - 1\right\} - \frac{V+IR_S}{R_{SH}} \quad (5)$$

The proposed circuit is focused on higher power applications. The inductors L_1 and L_2 are probable to operate under continuous conduction mode (CCM), hence the peak inductor current can be alleviated along with less conduction losses on active power switches. In CCM operation, the inductances of L_1 and L_2 are related only to the current ripple specification. Inductances of L_S dominates the output power range and ZVS operation.

Fig 2 shows the proposed soft switching converter system. Inductor L_1, MOSFET active power switch S_1, and D_1 diode comprise one step-up conversion unit, while the components S_2 and D_2 forms the other one. D_{sx} and C_{sx} are the intrinsic anti-parallel diode and output capacitance of MOSFET S_x respectively. The input voltage source V_{in}, via the two paralleled converters, replenishes output capacitor C_0 and the load.

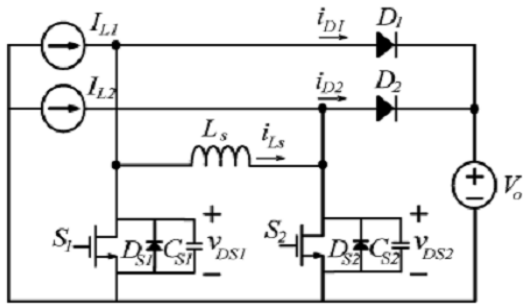

Fig 2. Proposed soft switching converter module

Inductor Ls is shunted with the two active power switches to release the electric charge stored within the output capacitor C_{sx} prior to the turn ON of S_x to ful fill zero-voltage turn ON (ZVS), and therefore, raises the converter efficiency.

III. OPERATION OF BOOST CONVERTER

Before examining on the circuit, the following assumptions are presumed.

1) The output capacitor C_0 should be large enough to neglect the output voltage ripple.

2) The forward voltage drops across MOSFET $S1$, $S2$ and diodes $D1$, $D2$ are neglected.

3) Inductors $L1$, $L2$ have large inductance and their currents are identical constants, i.e., $L1 = L2 = I_L$.

4) Output capacitances of switches C_{s1} and C_{s2} have the same values, i.e. $C_{S1} = C_{S2} = C_S$

5) The two active switches S1 and S2 are operated with pulse width modulation (PWM) control techniques. They are triggered with identical frequencies and duty ratios. Rising edges of the two gating signals are separated apart for half of the switching cycles. The complete operation of the converter can be divided into eight modes, the equivalent circuits and theoretical waveforms are shown in Fig 3 and Fig 4 respectively.

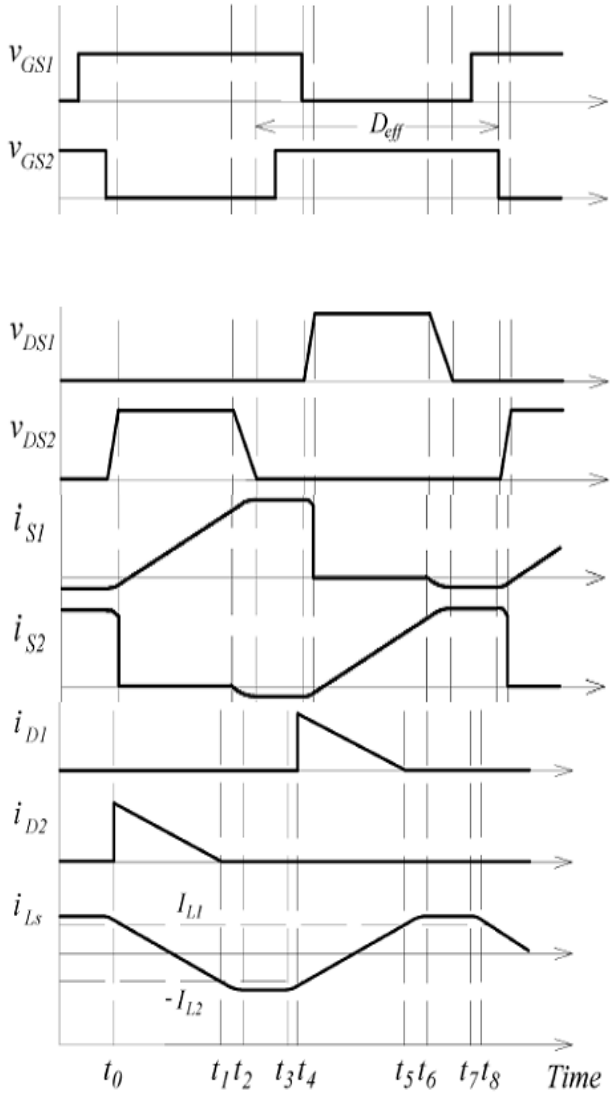

Fig 3. Theoretical waveforms of Boost Converter

A. Mode I :{ $t_0 < t < t_1$ referring to Fig 4.1}

Prior to this mode, the gating signal for switch $S2$ has already transited to low state and the voltage v_{DS2} rises to V_0 at t_0. At the beginning of this mode, current flowing through $S2$ completely commutates to D_2 to supply the load. Current i_{S1} returns from negative value toward zero; I_{L1} flows through Ls. Due to the zero voltage on v_{DS1}, the voltage across inductor Ls is V_0, i.e. i_{Ls} will decrease linearly at the rate of V_0/Ls. Meanwhile, the current flowing through S1 ramps up linearly.

As i_{Ls} drops to zero, current i_{S1} contains only i_{L1} while i_{D2} equals. The current I_{L2} and current I_{LS} will reverse its direction and flow through S1 together with $I_{L1.}$ As i_{LS} increases in negative direction, i_{D2} consistently reduces to zero. At this moment i_{LS} equals I_{L2} diode D_2 turns OFF, and thus this mode comes to an end.

Despite the minor deviation of i_{S1} from zero and i_{Ls} from i_{L1} currents, i_{Ls} i_{S1} i_{D2} and the duration of this mode 1 can be approximated as

$$i_{ls}(t) = I_L - \frac{V_0}{L_s}t$$

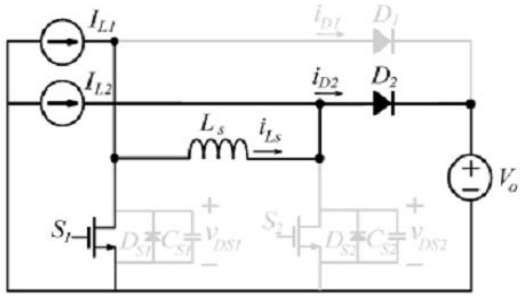

Fig 4.1

$$i_{s1}(t) = \frac{V_0}{L_s}t$$

$$i_{D2}(t) = 2I_L - \frac{V_0}{L_s}t$$

$$t_{01} = \frac{\left(\frac{3}{4} - D_{eff}\right)T_S - \sin^{-1}\left(V_0 \Big/ \left(V_0 + \frac{2I_L}{\omega C_S}\right)\right)}{\omega}$$

Where D_{eff} is the effective duty ratio to be explained later and $\omega = 1/\sqrt{L_S C_S}$

B. Mode II {$t_1 < t < t_2$, referring to Fig 4.2}

Whereas diode D_2 stops conducting, capacitor C_{s2} is not clamped at V_0 anymore. The current flowing through L_s and i_{Ls} continues increasing and commences to discharge C_{s2}. This mode will terminate as voltage across switch S_2, v_{DS2} drops to zero. Voltage v_{DS2} and current i_{ls} can be equated as

$$v_{DS2}(t) = V_0 \cos\omega(\omega t)$$

$$I_{Ls}(t) = -V_0\,\omega C_S \sin(\omega t) - I_L$$

$$t_{12} = \frac{\pi}{2\omega}$$

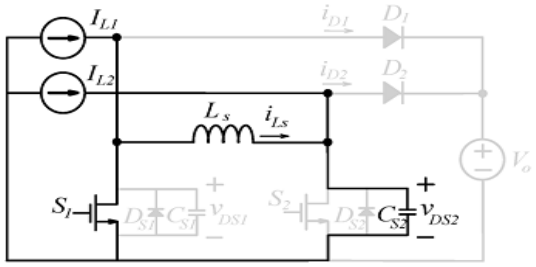

Fig 4.2

C. Mode III {t2 < t < t3, referring to Fig 4.3}

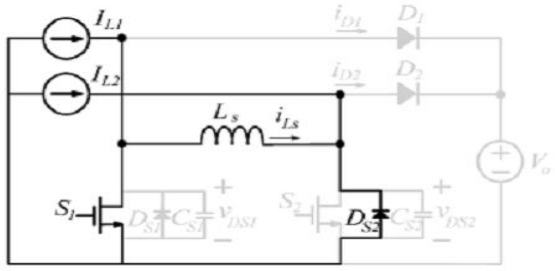

Fig 4.3

At t = t_2, voltage v_{DS2} decreases to zero. After this instant D_{s2}, the anti-parallel diode of S_2 begins to conduct current. The negative directional inductor current i_{ls} freewheels through S_1 and D_{s2}, and holds at a magnitude that equals $i_{ls}(t2)$ a little higher than I_L. During this mode, the voltage on switch S_2 is clamped to zero, and it is adequate to gate S_2 at zero-voltage turn ON.

D. Mode IV {t_3 < t < t_4, referring to Fig 4.4}

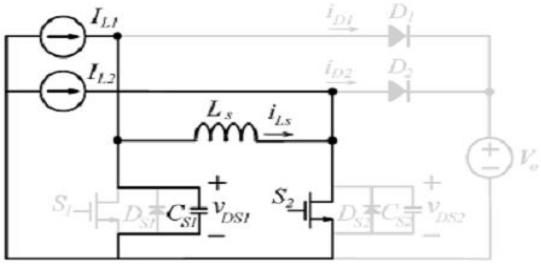

Fig 4.4

The switch S_1 turns OFF at t = t_3. Current i_{LS} begins to charge the capacitor C_{S1} the charging current includes i_{LS} and I_{L1}. Since the capacitor C_{S1} retrieves a little electric charge, i_{LS} decreases a little and resonates toward $-I_{L2,}$ In fact, I_{LS} will not equal $-I_{L2,}$ at i_{LS} even with a slightly higher magnitude. However, by ignoring the little discrepancy, the voltage on switch S_1 and current through L_S can be approximated as while the capacitor voltage v_{CS1} ramps to V_0, D_1 will be forward biased, and thus this mode will come to an end.

Modes I-IV describes the scenario of switch S_2 between OFF-state proceeding to ZVS turn -ON. Operations from modes V-VIII are the counterparts for switch S_1 due to the similarity, hence they are omitted here.

IV. SIMULINK MODEL

As stated above the whole circuit is the combination of photovoltaic cell and an efficient DC-DC boost converter, boost the small DC voltage to desired level. Here the MOSFET is replaced by IGBT/DIODE, has less switching losses. The complete simulink model is shown in fig 5.

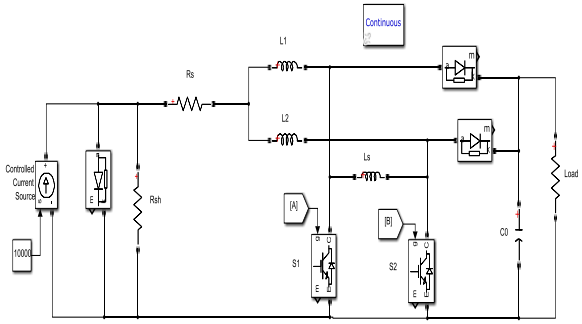

Fig 5. Simulink model of an Efficient Boost Converter

The parameters of the circuit is given in the table shown below.

Table: CIRCUIT PARAMETER

Parameters	Values
Shunt Resistance (R_{sh}) PV Cell	0.001Ω
Series Resistance (R_s) PV Cell	10000Ω
Inductors L_1 & L_2	300µH
Output Capacitor	330µF
Inductor L_S	270µH
Input Voltage	18.77V
Input Power	86W
Output Power	83.55W
Switching Frequency	20KHz

V. RESULTS

The theoretical result is shown in fig 3 and the simulation result is shown in fig 9. The simulation result is almost equal to the theoretical results. The input voltage is achieved by photovoltaic cell and this PV voltage is boosted and with the help of an efficient Boost converter the small voltage is boosted.

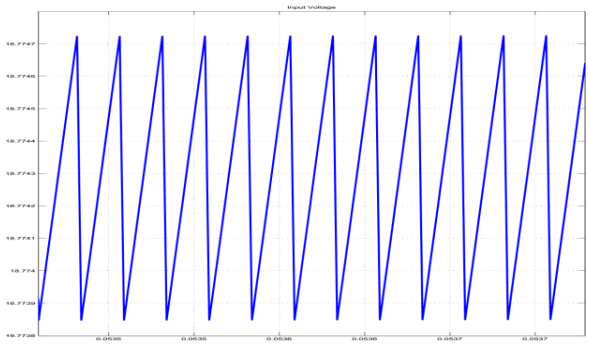

Fig 6. Input voltage ripple contents

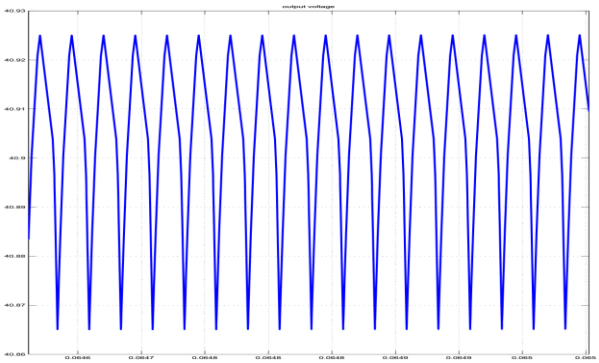

Fig 7. Output voltage ripple contents

The ripple contents of input voltage and output voltage is shown in fig 6 and 7 respectively.

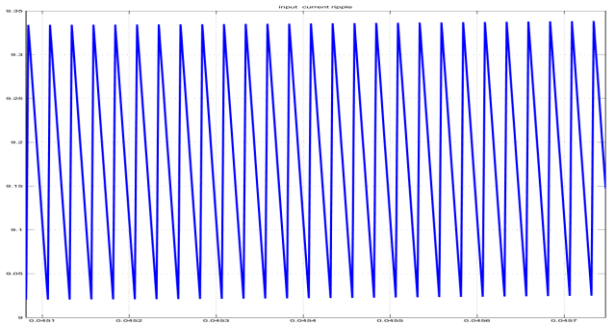

Fig 8. Input Current ripple

The ripple present in input current is very low, can be seen in fig 8.

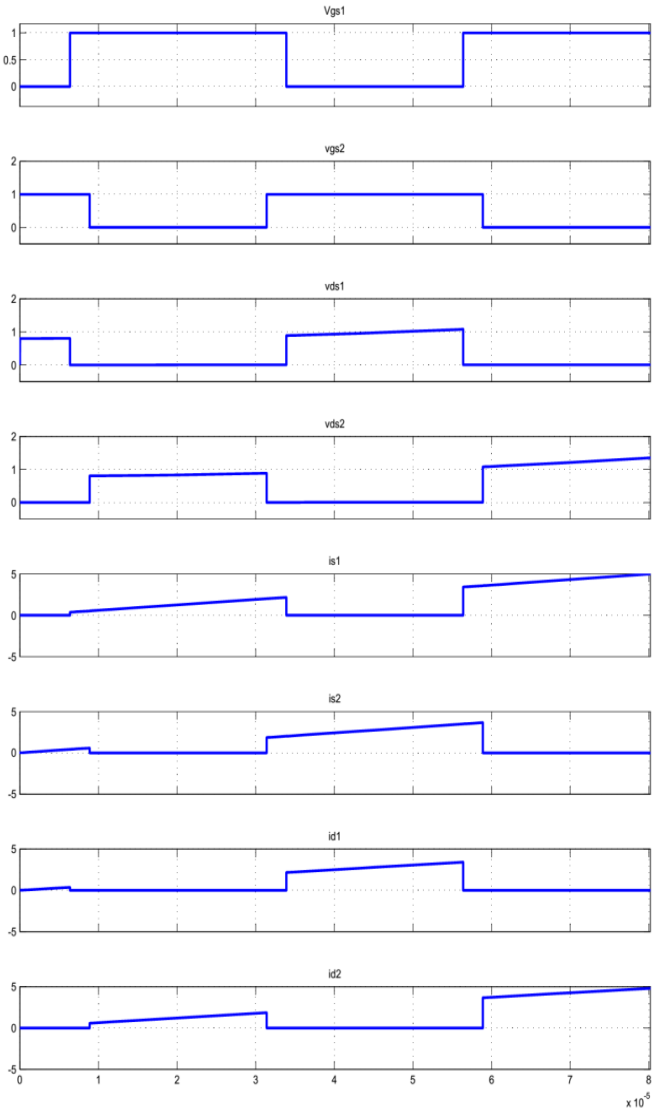

Fig 9. Simulation results across components

Here shown the input power and output power of the circuit, which have 97% efficiency. Since the input power is 86Watt and output power is 83.55Watt. Fig 10 showing the input and output power of the circuit.

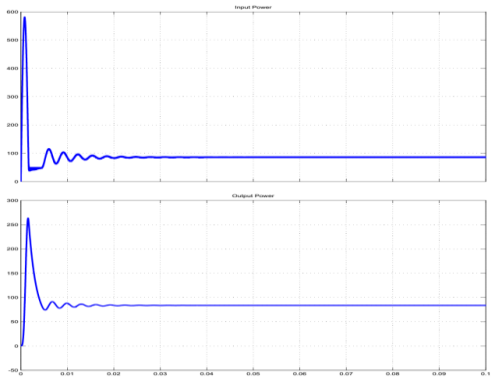

Fig 10. Input Power 86W & Output Power 83.55W

VI. CONCLUSION

This paper has proposed a dual boost converter with zero voltage turn-on. It inherits the merits of interleaved converters, i.e. low output voltage ripple. The detail analysis has presented the design and control equations. Inductor determines the performance of the converter. The converter can be controlled by varying switching frequency to deal with the fluctuation of input voltage and output load. In simulation result, the circuit efficiency achieves 97% at 83.55W output for input power 86W due to its ZVS characteristics.

REFERENCES

[1] Y. Jang, D. L. Dillman, and M. M. Jovanovic, "A new soft-switched PFC boost rectifier with integrated flyback converter for stand-bypower," IEEE Trans. Power Electron., vol. 21, no. 1, pp. 66–72, Jan.2006.

[2] K. Kobayashi, H. Matsuo, and Y. Sekine, "Novel solar-cell power supply system using a multiple-input DC–DC converter," IEEE Trans. Ind. Electron., vol. 53, no. 1, pp. 281–286, Feb. 2006.

[3] Y. Gu, Z. Lu, Z. Qian, X. Gu, and L. Hang, "A novel ZVS resonant reset dual switch forward DC–DC converter," IEEE Trans. Power Electron. , vol. 22, no. 1, pp. 96–103, Jan. 2007.

[4] C. J. Tseng and C. L. Chen, "A passive lossless snubber cell for non isolated PWM DC/DC converters," IEEE Trans. Ind. Electron., vol. 45, no. 4, pp. 593–601, Aug. 1998.

[5] F. W. Combrink, H. T. Mouton, J. H. R. Enslin, and H. Akagi, "Design optimization of an active resonant snubber for high power IGBT converters," IEEE Trans. Power Electron., vol. 21, no. 1, pp. 114–123,Jan. 2006.

[6] Yao-Ching Hsieh, Member, IEEE, Te-Chin Hsueh, and Hau-Chen Yen, "An Interleaved Boost Converter With Zero Voltage Transition", IEEE TRANSACTIONS ON POWER ELECTRONICS, VOL. 24, NO. 4, APRIL 2009.

[7] W. Li, J. Liu, J. Wu, and X. He, "Design and analysis of isolated ZVT boost converters for high-efficiency and high step-up applications," IEEE Trans. Power Electron., vol. 22, no. 6, pp. 2363–2373,Nov.2007.

AUTHORS

First Author – Nisha Singh, Dept. of Electrical Engineering SATI, Vidisha, Madhya Pradesh, India
Second Author – S. P. Phulambrikar, Associate Professor & HOD, Dept. of Electrical Engineering, SATI, Vidisha, Madhya Pradesh, India